Lung Region Segmentation Using Modified U-Net Architecture

Zhakaw Hamza Hamad[1] & Taban Fouad Majeed[2]

[1&2] Computer Science Department, College of Science, Salaheddin University, Erbil, Iraq
Correspondence: Zhakaw Hamza Hamad, Computer Science Department, College of Science, Salaheddin University, Erbil, Iraq.
Email: zhakaw.hamad@su.edu.krd

Doi: 10.23918/eajse.v8i3p25

Abstract: In order to combat the continuing COVID-19 pandemic, early infection diagnosis is essential. Lung infections can be detected using a screening technique called chest X-ray imaging (CXR). During pandemics, integrating machine learning techniques with medicine analysis is crucial in relieving the enormous load on healthcare systems and clinicians. As the continuing COVID-19 crisis intensifies in countries with dense populations and few testing kits, radiological Imaging can serve as a crucial diagnostic tool to properly classify covid-19 patients and administer the appropriate medication on time. In light of this objective, we describe our Research on segmenting lung areas utilizing a deep learning architecture and chest X-ray images as the source material. We used 2 public datasets, Montgomery & Shenzhen and Covid-Qu dataset. Also, the Research created the KURD-covid dataset and collected 1300 x-ray images from local health care centres that contain two labels, covid-19 and normal x-ray with manual masks for all images. We proposed the segmentation model based on state-of-art U-Net architecture. The result of the Covid-Qu daset was., %97 IoU and %99.5 DSC, and in KURD-covid is %71 IoU and %82 DSC.

Keywords: Deep Learning, Convolutional Neural Network, Segmentation, U-Net, Covid-19, X-Ray Images

1. Introduction

The newly discovered corona-virus infection 2019, also known as the COVID-19 outbreak, was discovered before the end of 2019 in Wuhan, and since then, it has swiftly spread throughout the world (Zhu et al., 2020).. The severe acute respiratory syndrome coronavirus is the causative agent of COVID-19, an infectious sickness. COVID-19 is characterized by fever, dry cough, and shortness of breath. Of breath, exhaustion, and a variety of other symptoms.

Before the vaccine came out, For COVID-19, no specific treatment was beneficial. As a result, precise and speedy testing is critical for the timely prevention of COVID-19 dissemination. Reverse transcriptase polymerase chain reaction (RT-PCR) is the most often used method of testing COVID-19. In contrast, RT-PCR testing requires significant time investment and is bound by a limited supply of test kits(Shan et al., 2020).

Furthermore, this method has been found to have limited sensitivity and recurrent failures. Testing is often required to confirm a COVID-19 case properly. According to this, many cases will not be verified quickly(C. Long et al., 2020),(Ai et al., 2020),, As a result, there is a greater danger of infecting a broader population. Moreover, few studies(Ai et al., 2020),(Salehi, Abedi, Balakrishnan, & Gholamrezanezhad, 2020),(Fang et al., 2020)If the RT-PCR findings for suspected individuals experiencing symptoms of shortness of breath or other respiratory issues were found to be negative, CT should be conducted as a secondary test.

Received: August 9 2022
Accepted: December 1, 2022
Hamad, Z.H., & Majeed, T.F. (2022). Lung Region Segmentation Using Modified U-Net Architecture. *Eurasian Journal of Science and Engineering*, *8*(3), 25-38.

CT scans, notwithstanding their enhanced performance, have obstacles and limits. Their sensitivity for early COVID-19 patients is weak. They have a slow image collection, are less useful, and are expensive. In contrast, X-ray images are a less costly, faster, and more widely available technology that exposes the body to less damaging radiation than CT(Brenner & Hall, 2007). In COVID-19 screening, Imaging of the chest utilizing a chest X-ray, also known as a CXR, is utilized often as a diagnostic aid. Furthermore, it is said to have a good predictive ability(Shi et al., 2020).

For evaluating COVID-19 infection in X-ray, precision in segmenting certain essential radiographic features is necessary. Medical imaging segmentation must get manual annotations from highly competent radiologists with specific training. The constantly rising number of persons who are infected with the disease. It has imposed a major burden on radiologists and inhibited ground-truth mask labelling labeling (Ai et al., 2020; Gaál, Maga, & Lukács, 2020).

Image segmentation is an essential component of computer vision and image processing, playing an important part in a broad range of applications, including scene interpretation, medical image analysis, robotic perception, video surveillance, augmented reality, and image compression(Minaee et al., 2021). In radiology research and clinical practice, image segmentation, in general, has developed into a role that is becoming increasing amount more significant. Segmentation aims to isolate areas of interest from other body portions so that quantitative measurements may be taken. In addition, they are specifically gaining additional diagnostic information, such as evaluating the area and volume of segmented structures.

Many researchers have recently published Deep Learning techniques for automating corona-virus identification from x-ray Images.(Ozturk et al., 2020),(Apostolopoulos & Mpesiana, 2020),(Chowdhury et al., 2020). Researchers have shown great disease detection performance but also several difficulties and limitations. To begin with, they all employed a minimal quantity of COVID-19 data, with the biggest dataset being just a few hundred X-ray samples. As previously stated, such a paucity of data leads to a lack of thorough assessment, making it impossible to generalize their conclusions in reality. Furthermore, they were interested in Detection and classifying COVID-19, among other kinds, with no additional segmentation or localization. Because of these limitations, its applicability and robustness for clinical use will be severely restricted. However, few investigations have been conducted(Oh, Park, & Ye, 2020),(Rajaraman et al., 2020).The initial step in their detecting technique was lung segmentation. This promotes accurate categorization decision-making and protects the lungs from other parts of the body that are not vital to breathing. CXR images of varying quality are used to train previous segmentation methods, on the other hand., mostly from Montgomery(Jaeger et al., 2013) and Shenzhen (Candemir et al., 2013). The initial step in their detecting technique was lung segmentation. A network's ability to accurately categorize and defend itself from non-pulmonary like the heart, bones, backdrops, or text is enhanced by this method. However, early segmentation methods were trained on various materials ranging from low to high grade. Chest x-ray, mostly from Montgomery. Creating KURD-covid chest x-ray datasets that contain ground truth masks for accurate lung segmentation is essential. It will assist researchers and physicians in providing a more accurate segmentation system for COVID-19 and other lung disorders.

Masks for the ground-truth segmentation of the lungs. Full KUED-covid datasets were constructed for the first time utilizing a 3D slicer tool mentioned in(Alnaser, Gong, & Moeller, 2016), one of the finest applications for producing masks in medical image segmentation collaborative technique that considerably minimizes human labour to annotate the images. As part of this initiative, the data and ground-truth masks will be made available to the g public dataset. We hope the KURD-covid dataset will be incredibly useful for academics, clinicians, and students.

Throughout the globe to develop creative strategies for the Detection of COVID-19 at an early stage using excellent benchmark X-ray images obtained from COVID-19 and ground-truth lung masks. We also proposed a segmentation model to segment lung regions on chest x-ray images based on U-Net for segmenting biomedical images and adapting basic U-Net for lung segmentation tasks. - Finally, we presented a unique and robust approach for lung segmentation using CXR images. As shown in figure (1), This is a critical achievement for the most accurate diagnosis and evaluation of the condition yet achieved.

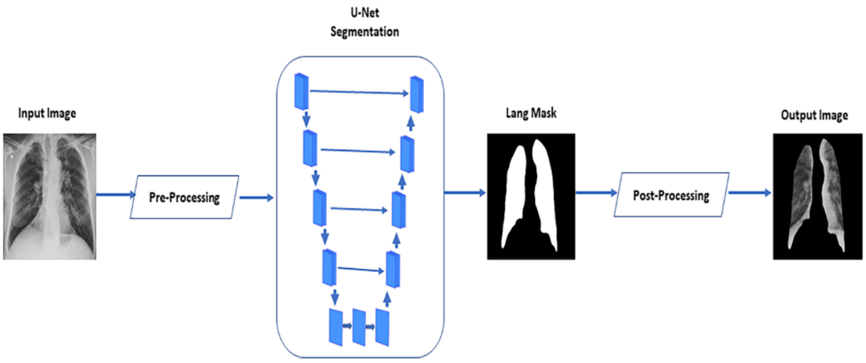

Figure1: methodology of the predicting lung mask using U-Net with preprocessing and post-processing

2. Related Work

Deep Learning in image segmentation, focusing on computer vision and medical Imaging, has become one of the most prominent disciplines of study in recent years(Oh et al., 2020)Medical diagnosis has made extensive use of computer vision(Oulefki, Agaian, Trongtirakul, & Laouar, 2021)Modern image segmentation models are versions of the encoder-decoder architecture, such as U-Net, a sort of fully convolutional network developed by(Ronneberger, Fischer, & Brox, 2015) and a full convolutional network (FCN) (J. Long, Shelhamer, & Darrell, 2015)However, the essential organ for our study is the lung, and we will discuss several studies that work to segment lung area authors in this section. (Rashid, Akram, & Hassan, 2018).To segment, the lung area from CXR images, utilize a fully convolutional network. Moreover, the flood fill holes method was post-processed to determine the typical level of precision. The strategy was evaluated using three datasets: one from the Japanese Society of Radiological Technology (JSRT), one from Montgomery County (MC), and one from a local dataset. The approach achieved an average accuracy of 97.1 per cent, 97.7 per cent, and 94.2 per cent, respectively, across the three datasets. Another work is is (Frid-Adar, Ben-Cohen, Amer, & Greenspan, 2018). The Encoder used pre-trained VGG-16 architectures, while the decoder used sampling and normal convolution to segment a chest radiograph's lungs, heart, and clavicles. The authors also examine the influence of loss functions on neural network training for semantic segmentation. The dataset includes 247 CXR images from JSRT and SCR segmentation masks. The optimal architecture was a U-Net updated with pre-trained encoder weights, with IoU of 96.1 for lung fields, 90.6 for the heart, and 85.0 for the clavicles.(Li, Kang, Cheng, & Zhang, 2019)CNN model for detecting pneumonia CNN deletes and labels the image's pneumonia area as a non-pneumonia sample to focus on the disease-specific region. Transfer learning separates the lung interest region to reduce background noise. T(IoU) accuracy was 0.262. Lung segmentation has numerous goals. The U-Net is a regularly utilized technique in COVID applications to segment lung areas and lesions.

(Arias-Garzón et al., 2021). Using existing deep learning models (VGG19 and U-Net), these images are processed and classified if COVID-19 is positive or negative. Regarding DSC, the segmentation results of train and validation were around per cent 98 and per cent 96, respectively, while IoU was trained per cent 95 validation per cent 90. Also (Tahir et al., 2021), segmented lungs, localized COVID-19, and quantified infection from chest x-rays. 33,920 x-rays and 11,956 COVID-19 samples with segmentation masks were employed. Feature Pyramid, U-Net++, and U-Net were used (FPN). After a long iterative procedure, the constructed network segmented lung areas with 96.11 IoU and 97.99 DSC. 83.05 per cent IoU and 88.21 per cent DSC localized COVID-19 infections.

Another research (Bassi & Attux, 2021) suggested a DNN to segment and classify lungs, Stacking U-Net, intermediate, and classification modules (DenseNet201). They created performance indicator probability distributions using external data and Bayesian inference. Their DNN got a 0.917 AUC on an external test dataset, whereas a DenseNet without segmentation achieved a 0.906 AUC. Bayesian inference showed 76.1% accuracy and [0.695, 0.826] 95 percent HDI with segmentation and 71.7% and [0.646, 0.786] without segmentation.

Here Also, researchers (Teixeira et al., 2021) assess COVID-19 identification utilizing a lung segmentation x-ray image. The authors used a U-Net CNN architecture for semantic segmentation and three CNN architectures for classification (VGG, ResNet, and Inception). They were estimating segmentation's impact on AI. Pneumonia, lung opacity, and COVID-19were included in a database. They evaluated the impact of constructing chest x-ray image datasets from multiple sources and generalizing COVID-19. The segmentation was 0.034 Jaccard and 0.982 Dice. The segmented image classification The multi-class score was 0.88, while the COVID-19 score was 0.83. Using segmented CXR, an F1-Score of 0.74 and an AUC of 0.9 was achieved for COVID-19 diagnosis in the cross-dataset scenario. Also, in (Gopatoti & Vijayalakshmi, 2022), COVID-19 infected lung lobes will be marked on CXR images in this study to distinguish COVID-19 from healthy individuals. For COVID-19 early detection, SegNet, U-Net and a hybrid CNN utilizing SegNet and U-Net are recommended for segmenting infected lung lobes from CXR images. Sophisticated CXR image semantic segmentation networks may be built using Grey wolf optimization (GWO). The best CXR image semantic segmentation networks for COVID-19 image identification yielded a 92% success rate. ' With an accuracy of 98.08 per cent, SegNet trumps optimized U-Net and hybrid CNN in the segmentation and classification of COVID-19 infected airways.

However (Štifanić et al., 2021).This study used DeepLabv3+ with Xception 65, MobileNetV2, and ResNet101 for lung segmentation. The recommended strategy generated an average IoU of 0.910. The F1 value was 0.925, the accuracy was 0.968, the precision was 0.916, the sensitivity was 0.935, and the specificity was 0.977.

In (An, Cai, Qu, & Gao, 2021),They proposed a multi-appearance COVID-19 screening framework using chest x-ray lung area priors. To improve cross-domain lung segmentation, they propose an adversarial adaptation network for several scales (MS-AdaNet). Using lung region priors, they create a three-subnetwork multi-appearance network (MA-Net) for feature extraction and fusion. Researchers can predict MA-Net was used to treat normal viral pneumonia and COVID-19 infections. MS-AdaNet lung segmentation is expanded using three available CXR datasets. MS-AdaNet outperforms contrastive lung segmentation techniques, the study found. On COVID-19 screening, MA-Net achieves 98.83% accuracy and 98.71% F1 score.

3. Datasets

We used two published datasets to verify our lung segmentation work and created the KURD-covid dataset. The public datasets included 138 images from Montgomery with their associated ground truth masks and 566 images from Shenzhen(Candemir et al., 2013) (Jaeger et al., 2013)

and covid-Qu dataset (Tahir et al., 2021) 33,000 images, 11,956 covid, 11,263 non-covid (infected x-ray) (viral, pneumonia), and 10 701 normal (healthy)

KURD-covid dataset, we collected images from most of the health centres and hospitals in Erbil and obtained 1300 images, 613 images of covid-19 and 687 images of normal healthy images. The size of the images we resized was 512x512, and the ground truth mask was created manually by a 3D slicer application under the supervision of radiologists. Also, our dataset was verified by radiologists.

The process of creating manual masks has been started under supervision of a special radiologist,later he checked all masks to see the efficiency of the accomplished work.Finally he compare all masks with original x-ray individually, to see the accuracy of the manual mask.

3. Methods and Materials

3.1 Preprocessing Step

All X-ray images are resized into 512*512 dimensions because all images come from different resources and sizes. In addition, we cropped some images because most images have a black frame and a morphological process that was dilation and counter, that detect edge and precise edge point.

However, we do some filters like histogram equalization. After that, the images go into Network architecture to predict lung masks. Finally, for better visualization, we do some post-processing like region prop that removes unwanted objects after predicting mask.

3.2 U-Net

The most advanced models for image segmentation are versions of the encoder-decoder architecture, such as U-Net, a form of fully convolutional network proposed.(Ronneberger et al., 2015), in addition to the fully convolutional network (FCN) (J. Long et al., 2015)The conventional U-Net is an artificial neural network (ANN) with convolutional and deconvolutional layers for biomedical image segmentation. U-Net is a symmetrical network composed of an encoder and decoder are the two components that make up the whole. The function of the Encoder is to extract spatial information from the primary medical records. Moreover, Using the extracted spatial features, the decoder is to generate the segmentation map. Meanwhile, using many convolutional layers, the Encoder adopts a similar structure to FCN. U-Net is dedicated to solving more problems. It can localize and distinguish borders because classification is performed on each pixel; when the number of annotated samples is low, it functions effectively through substantial data augmentation. The feature maps in the expansion path are mixed with features retrieved at different levels in the contraction path. Resulting in a larger number of features that are required for accurate segmentation.

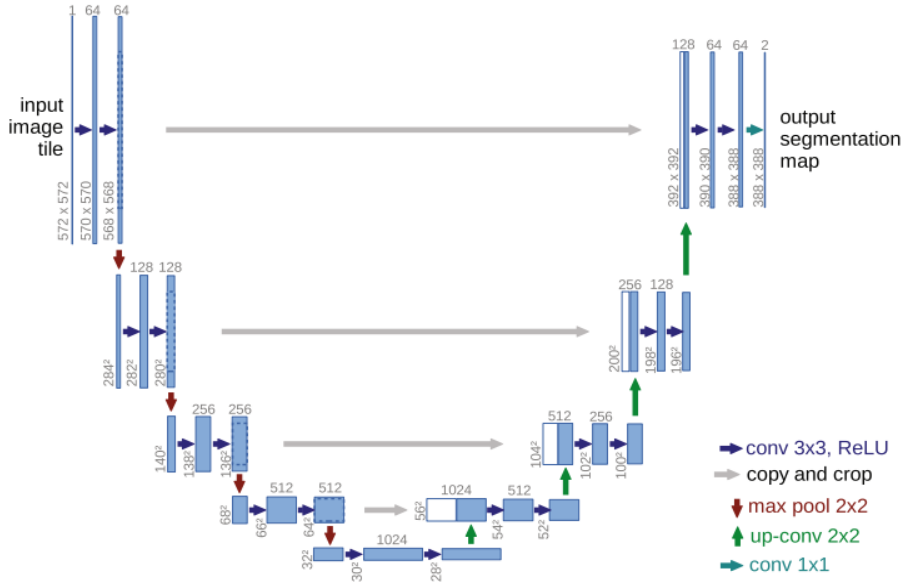

Figure 2: basic U-Net architecture

3.3 Proposed Method

Each block has two 3x3 convolution layers (the same padding), and the Max pooling is 2x2 and stride 2 to do down-sampling operations. There were 32 feature channels available at launch. Convolutional layers have two blocks added to the baseline U-net every time they are down-sampled. The Encoder connects to the decoder using two 3x3 convolutional layers. In contrast to the Encoder, the decoder is designed for image upsampling and segmentation. As a result, the encoder-generated feature map is first up-sampled by the decoder using a 2×2 deconvolutional layer. After then, the deconvolutionary layer emerged as a result of of (Zeiler, Krishnan, Taylor, & Fergus, 2010). As a result, there are just half as many output filters as there were before. There are then two 3x3 convolution layers and one deconvolution layer in a sequence of up-sampling blocks. In order to obtain the segmentation result, the final layer is a 1 x 1 convolutional layer (see figure 2). Finally, the last layer used the Sigmoid function as its activation function instead of ReLU.

Functions such as ReLU and Sigmoid are described as follows:

$$ReLU = \ f(x) = \max(0, x) \tag{1}$$

$$Sigmoid = \ f(x) = \frac{1}{1+exp(-x)} \tag{2}$$

U-Net also integrates some of the encoder and decoder functionalities into a single unit in the Encoder, before max-pooling, the convolution output for each block is symmetrically transferred to the decoder for processing. Each decoder block receives the Encoder's learned feature representation and adds it to the deconvolutional layer's output. The result of the concatenation is then sent to the next block. To help the decoder recover features that may have been lost owing to max-pooling, this concatenation step is beneficial.

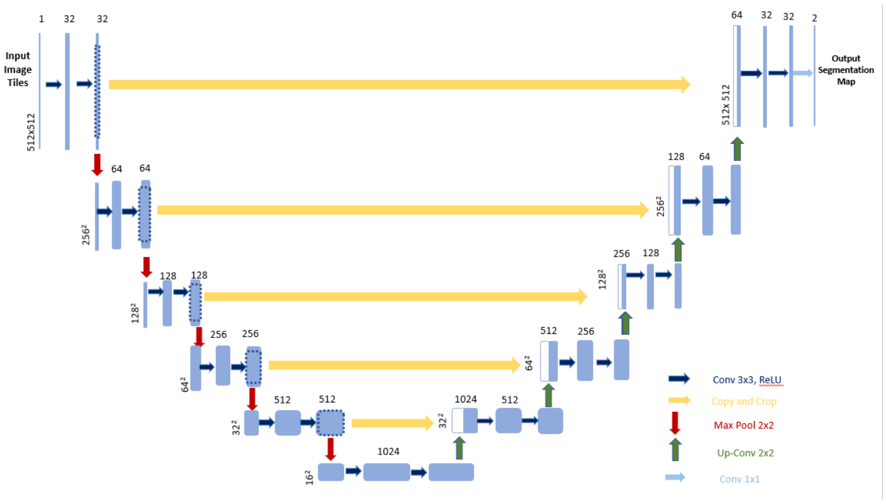

Figure 3: the architecture of the proposed method

4.3-Evaluation Matrices

To test our lung segmentation model, we employed the following evaluation matrices: Intersection Over Union, Dice Similarity Coefficient, and Precision

$$Recall = \frac{TP}{TP+FN} \quad [3]$$

$$Precision\frac{TP}{TP+FN} \quad [4]$$

$$DSC = \frac{2TP}{2TP+FP+FN} \quad [5]$$

$$DSC = \frac{2TP}{2TP+FP+FN} \quad [6]$$

That TP=True Positive, FN=False Negative, FP=False Positive

5. Experimental Steps Results

The experiments This section discusses our model that plan is segmented lung region was trained and evaluated by basic U-net and modified U- Net, the training parameters in the model are as follows the number of epoch =40, mini-batch size =2, initial learning rate =1e-5, all experimenting conducting using python (9) on core i7 9th Gen, GPU machine, Nvidia GeForce GTX1600 Ti with Max-Q-Design with 18 GB of RAM, Figure 3,4 compares the results of the two networks to the ground truth. Both networks can consistently segment not only incidences of COVID-19 pneumonia but also cases of pneumonia not caused by COVID-19, with varying degrees of severity; this is an intriguing discovery.

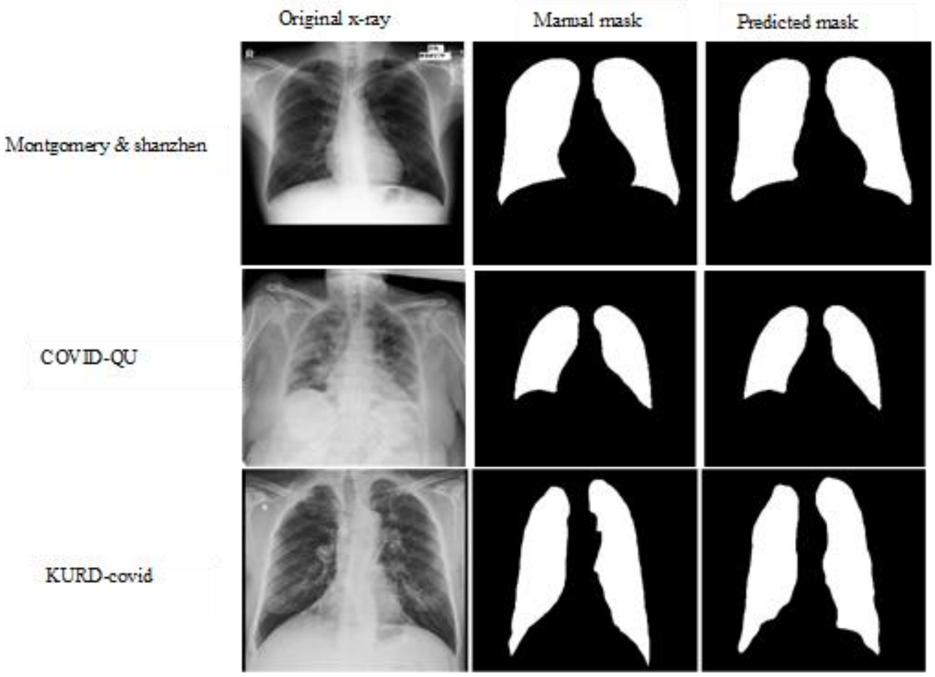

Figure 4: x-ray samples with manual mask and predicted mask from basic U-net for three datasets

The 33,000 CXR samples from COVID-19, non-COVID-19, and regular courses were used to create this exquisite performance. That we used three datasets after testing two public datasets, as the results of unseen samples are shown in table (1), it was declared that the result in the proposed method is better than the basic U-Net of both covid-Qu and KURD-covid datasets. in Covid-QU the result in term IoU, DSC, Recall, precision, accuracy in basic U-net is %95.7, %97.8, %95.3, %96.8, %98 respectively however our model is: IoU is %97, DSC is %99.5, Recall is %097.9, precision is %99, accuracy is %99 And in KURD-covid in our model is better than basic U-net IoU, DSC, Recall, precision, accuracy was %66.4, %77.9, %77, %80, %92 Our-model is IoU, DSC, Recall, precision, accuracy, %71.8, %82.2, %80, %85.4, %94.2. the reason that we increase a layer in the encoder part is that it makes the number of training increase that also we increase another layer in the decoder part that precise better segmentation as we see the result.

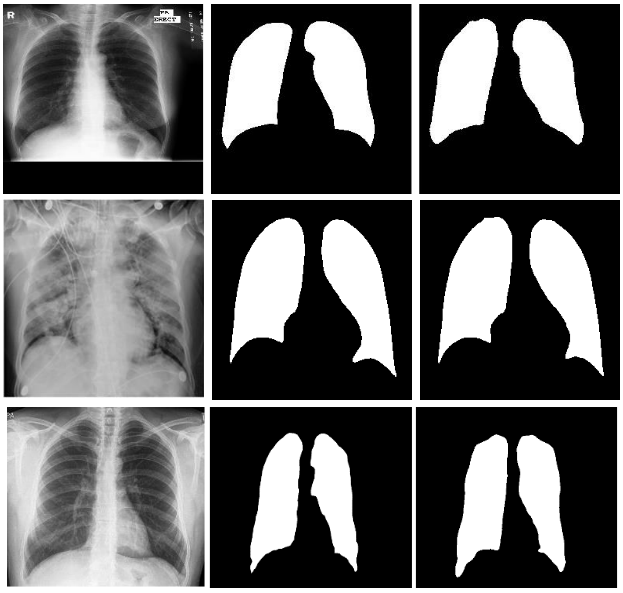

Figure 5: x-ray samples with manual mask and predicted mask from basic U-net for three datasets

Table 1: shows the result of unseen data for whole datasets after 40 epochs in Basic-U-Net architecture and modified U-net

Model	dataset	IoU	DSC	Recall	Precision	Accuracy
U-Net	Montgomery And shanhzen	0.9237	0.9596	0.9532	0.9682	0.9804
	Covid-QU	0.9576	0.9780	0.9786	0.9805	0.9900
	Kurd-covid	0.6648	0.7796	0.7708	0.8058	0.9285
Modified U-Net	Montgomery And shanzhen	0.9170	0.9559	0.9518	0.9627	0.9727
	Qu-covid	0.9705	0.9959	0.9799	0.9996	0.9956
	Kurd-covid	0.7184	0.8220	0.8058	0.8543	0.9425

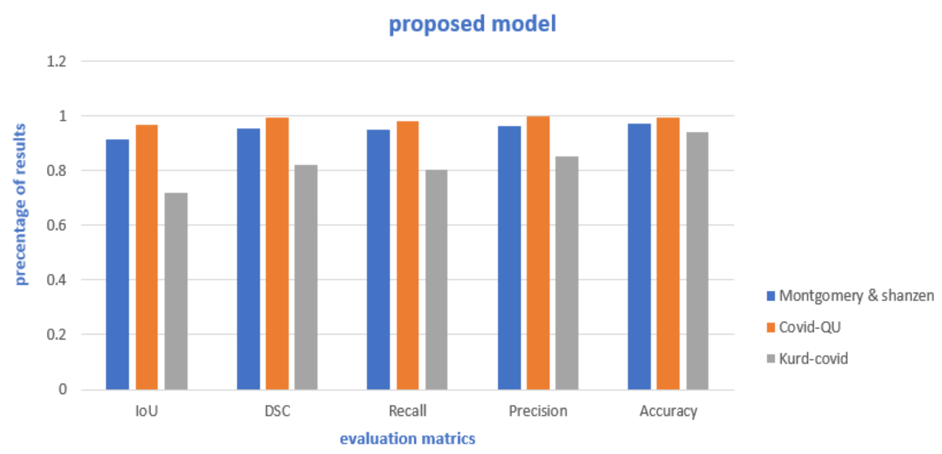

Figure 6: result of proposed model presented by chart

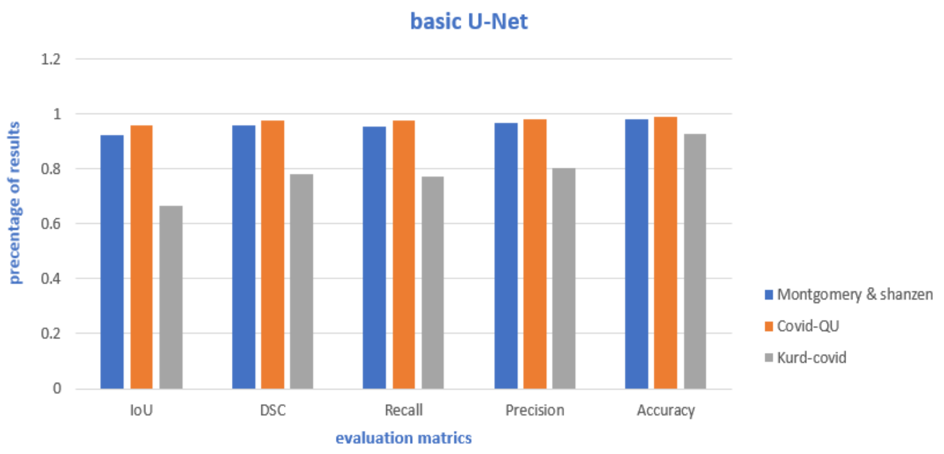

Figure 7: result of basic U-net presented by chart

Table 2: shows the result of training and validation of the whole dataset after 40 epoch epochs in basic-Unet architecture and modified U-net

Model	dataset	IoU	DSC	Recall	Precision
U-Net	Montgomery And shanzhen	0.9008	0.9473	0.9387	0.9677
	Qu-covid	0.9904	0.9811	0.9908	0.9901
	Kurd-covid	0.6591	0.7862	0.7973	0.8069

Modified U-Net	Montgomery And shanzhen	0.9115	83.87	0.9657	0.9344
	Qu-covid	0.9919	0.9840	0.9920	0.9922
	Kurd-covid	0.6980	0.8153	0.8240	0.8449

6. Discussion

The COVID-19 epidemic is worsening daily, and sufferers must be tested and diagnosed as soon as possible. So the study provides a brand-new idea.CNN model that we modify the state of art segmentation algorithm that was U-net for biomedical image segmentation, and we have an interesting result that illustrated in result section compare with other previews published articles,(Rahman et al., 2021)that used covqu dataset and modified U-net the result was %94.5 by DSC, and also (Tahir et al., 2021)creating a big dataset with COVQU named COVED-QU dataset the result by DSC %97.99 our model with COVED-QU dataset is %99.5, and also in the Research has comparestion to the proposed method with the basic U-Net for this study we create the local dataset with ground truth mask named KURD-covid dataset that the result illustrate in table 1 that the increase the presiceing segmentation more than %4 in term DSC and IoU that is an intrset value in medical , even finished covid-19 pandemic the researchers can use the model and the dataset for other lung diseases,the advantage of the proposed model is increse the presice segmentation that is very important in the medical domain because it has the relationship with human life , on another hand the disadvantage of the our model is increase the number of parameters however the increasing number of parameters didn't rise the time of traing but need using more gpu and hardware.

7. Conclusion

Identifying and isolating highly infectious COVID-19 cases as soon as possible is crucial for avoiding widespread infection by a virus. CXR imaging provides a low-cost, readily available, and quick alternative to established diagnostic procedures, including RT-PCR and computed tomography images. Many studies have consequently proposed AI-based solutions for automated and real-time COVID-19 analysis. Identification generally, the segmentation of lung regions makes disease classification and Detection simpler. This work presents a model system to partition the lung using CXR covid and normal patient images. To do this, we collect images from the majority of centres and hospitals in Erbil, and then, under the supervision of a radiologist, we develop a ground truth mask. The KURD-covid dataset contains 613 images of covid and 687 images of normal. The freely available Deep CNN analysis on a comparable dataset will allow researchers to develop a remedy for COVID-19 and other pulmonary pathology concerns that is more dependable. This is the data.

Reference

Ai, T., Yang, Z., Hou, H., Zhan, C., Chen, C., Lv, W., . . . Xia, L. (2020). Correlation of chest CT and RT-PCR testing for coronavirus disease 2019 (COVID-19) in China: a report of 1014 cases. *Radiology, 296*(2), E32-E40.

Alnaser, A., Gong, B., & Moeller, K. (2016). Evaluation of open-source software for the lung segmentation. *Current Directions in Biomedical Engineering, 2*(1), 515-518.

An, J., Cai, Q., Qu, Z., & Gao, Z. (2021). COVID-19 Screening in Chest X-Ray Images Using Lung Region Priors. *IEEE Journal of Biomedical and Health Informatics, 25*(11), 4119-4127.

Apostolopoulos, I. D., & Mpesiana, T. A. (2020). Covid-19: automatic detection from x-ray images utilizing transfer learning with convolutional neural networks. *Physical and Engineering Sciences in Medicine, 43*(2), 635-640.

Arias-Garzón, D., Alzate-Grisales, J. A., Orozco-Arias, S., Arteaga-Arteaga, H. B., Bravo-Ortiz, M. A., Mora-Rubio, A., . . . Cardona-Morales, O. (2021). COVID-19 detection in X-ray images using convolutional neural networks. *Machine Learning with Applications, 6*, 100138.

Bassi, P. R., & Attux, R. (2021). COVID-19 detection using chest X-rays: Is lung segmentation important for generalization? *arXiv preprint arXiv:2104.06176*.

Brenner, D. J., & Hall, E. J. (2007). Computed tomography—an increasing source of radiation exposure. *New England journal of medicine, 357*(22), 2277-2284.

Candemir, S., Jaeger, S., Palaniappan, K., Musco, J. P., Singh, R. K., Xue, Z., . . . McDonald, C. J. (2013). Lung segmentation in chest radiographs using anatomical atlases with nonrigid registration. *IEEE Transactions on Medical Imaging, 33*(2), 577-590.

Chowdhury, M. E., Rahman, T., Khandakar, A., Mazhar, R., Kadir, M. A., Mahbub, Z. B., . . . Al Emadi, N. (2020). Can AI help in screening viral and COVID-19 pneumonia? *IEEE Access, 8*, 132665-132676.

Fang, Y., Zhang, H., Xie, J., Lin, M., Ying, L., Pang, P., & Ji, W. (2020). Sensitivity of chest CT for COVID-19: comparison to RT-PCR. *Radiology, 296*(2), E115-E117.

Frid-Adar, M., Ben-Cohen, A., Amer, R., & Greenspan, H. (2018). Improving the segmentation of anatomical structures in chest radiographs using u-net with an imagenet pre-trained encoder *Image Analysis for Moving Organ, Breast, and Thoracic Images* (pp. 159-168): Springer.

Gaál, G., Maga, B., & Lukács, A. (2020). Attention u-net based adversarial architectures for chest x-ray lung segmentation. *arXiv preprint arXiv:2003.10304*.

Gopatoti, A., & Vijayalakshmi, P. (2022). Optimized chest X-ray image semantic segmentation networks for COVID-19 early detection. *Journal of X-Ray Science and Technology*(Preprint), 1-22.

Jaeger, S., Karargyris, A., Candemir, S., Folio, L., Siegelman, J., Callaghan, F., . . . Antani, S. (2013). Automatic tuberculosis screening using chest radiographs. *IEEE Transactions on Medical Imaging, 33*(2), 233-245.

Li, B., Kang, G., Cheng, K., & Zhang, N. (2019). *Attention-guided convolutional neural network for detecting pneumonia on chest x-rays.* Paper presented at the 2019 41st annual international conference of the ieee engineering in medicine and biology society (EMBC).

Long, C., Xu, H., Shen, Q., Zhang, X., Fan, B., Wang, C., . . . Li, H. (2020). Diagnosis of the Coronavirus disease (COVID-19): rRT-PCR or CT? *European journal of radiology, 126*, 108961.

Long, J., Shelhamer, E., & Darrell, T. (2015). *Fully convolutional networks for semantic segmentation.* Paper presented at the Proceedings of the IEEE conference on computer vision and pattern recognition.

Minaee, S., Boykov, Y. Y., Porikli, F., Plaza, A. J., Kehtarnavaz, N., & Terzopoulos, D. (2021). Image segmentation using deep learning: A survey. *IEEE Transactions on Pattern Analysis and Machine Intelligence*.

Oh, Y., Park, S., & Ye, J. C. (2020). Deep learning COVID-19 features on CXR using limited training data sets. *IEEE Transactions on Medical Imaging, 39*(8), 2688-2700.

Oulefki, A., Agaian, S., Trongtirakul, T., & Laouar, A. K. (2021). Automatic COVID-19 lung infected region segmentation and measurement using CT-scans images. *Pattern recognition, 114*, 107747.

Ozturk, T., Talo, M., Yildirim, E. A., Baloglu, U. B., Yildirim, O., & Acharya, U. R. (2020). Automated detection of COVID-19 cases using deep neural networks with X-ray images. *Computers in Biology and Medicine, 121*, 103792.

Rahman, T., Khandakar, A., Qiblawey, Y., Tahir, A., Kiranyaz, S., Kashem, S. B. A., . . . Khan, M. S. (2021). Exploring the effect of image enhancement techniques on COVID-19 detection using chest X-ray images. *Computers in Biology and Medicine, 132*, 104319.

Rajaraman, S., Siegelman, J., Alderson, P. O., Folio, L. S., Folio, L. R., & Antani, S. K. (2020). Iteratively pruned deep learning ensembles for COVID-19 detection in chest X-rays. *IEEE Access, 8*, 115041-115050.

Rashid, R., Akram, M. U., & Hassan, T. (2018). *Fully convolutional neural network for lungs segmentation from chest X-rays.* Paper presented at the International Conference Image Analysis and Recognition.

Ronneberger, O., Fischer, P., & Brox, T. (2015). *U-net: Convolutional networks for biomedical image segmentation.* Paper presented at the International Conference on Medical image computing and computer-assisted intervention.

Salehi, S., Abedi, A., Balakrishnan, S., & Gholamrezanezhad, A. (2020). Coronavirus disease 2019 (COVID-19): a systematic review of imaging findings in 919 patients. *Ajr Am J Roentgenol, 215*(1), 87-93.

Shan, F., Gao, Y., Wang, J., Shi, W., Shi, N., Han, M., . . . Shi, Y. (2020). Lung infection quantification of COVID-19 in CT images with deep learning. *arXiv preprint arXiv:2003.04655*.

Shi, F., Wang, J., Shi, J., Wu, Z., Wang, Q., Tang, Z., . . . Shen, D. (2020). Review of artificial intelligence techniques in imaging data acquisition, segmentation, and diagnosis for COVID-19. *IEEE reviews in biomedical engineering, 14*, 4-15.

Štifanić, D., Musulin, J., Jurilj, Z., Šegota, S., Lorencin, I., Anđelić, N., . . . Filipović, N. (2021). Semantic segmentation of chest X-ray images based on the severity of COVID-19 infected patients. *EAI Endorsed Transactions on Bioengineering and Bioinformatics, 1*, e3.

Tahir, A. M., Chowdhury, M. E., Khandakar, A., Rahman, T., Qiblawey, Y., Khurshid, U., . . . Al-Maadeed, S. (2021). COVID-19 infection localization and severity grading from chest X-ray images. *Computers in Biology and Medicine, 139*, 105002.

Teixeira, L. O., Pereira, R. M., Bertolini, D., Oliveira, L. S., Nanni, L., Cavalcanti, G. D., & Costa, Y. M. (2021). Impact of lung segmentation on the diagnosis and explanation of COVID-19 in chest X-ray images. *Sensors, 21*(21), 7116.

Zeiler, M. D., Krishnan, D., Taylor, G. W., & Fergus, R. (2010). *Deconvolutional networks.* Paper presented at the 2010 IEEE Computer Society Conference on computer vision and pattern recognition.

Zhu, N., Zhang, D., Wang, W., Li, X., Yang, B., Song, J., . . . Lu, R. (2020). A novel coronavirus from patients with pneumonia in China, 2019. *New England journal of medicine*.